Perturbation of Sarcoplasmic Reticulum Calcium Release and Phenol Red Absorbance Transients by Large Concentrations of Fura-2 Injected into Frog Skeletal Muscle Fibers

P. C. PAPE, M. KONISHI, S. HOLLINGWORTH, and S. M. BAYLOR

From the Department of Physiology, University of Pennsylvania Medical Center, Philadelphia, Pennsylvania 19104-6085

ABSTRACT Intact single twitch fibers from frog muscle were studied on an optical bench apparatus after micro-injection with two indicator dyes: phenol red, to monitor a previously described signal (denoted ΔpH_{app}; Hollingworth and Baylor. 1990. *J. Gen. Physiol.* 96:473–491) possibly reflective of a myoplasmic pH change following action potential stimulation; and fura-2, to monitor the associated change in the myoplasmic free calcium concentration ($\Delta[Ca^{2+}]$). Additionally, it was expected that large myoplasmic concentrations of fura-2 (0.5–1.5 mM) might alter ΔpH_{app}, since it was previously found (Baylor and Hollingworth. 1988. *J. Physiol.* 403:151–192) that the Ca^{2+}-buffering effects of large fura-2 concentrations: (*a*) increase the estimated total concentration of Ca^{2+} (denoted by $\Delta[Ca_T]$) released from the sarcoplasmic reticulum (SR), but (*b*) reduce and abbreviate $\Delta[Ca^{2+}]$. The experiments show that ΔpH_{app} was increased at the larger fura-2 concentrations; moreover, the increase in ΔpH_{app} was approximately in proportion to the increase in $\Delta[Ca_T]$. At all fura-2 concentrations, the time course of ΔpH_{app}, through time to peak, was closely similar to, although probably slightly slower than, that of $\Delta[Ca_T]$. These properties of ΔpH_{app} are consistent with an hypothesis proposed by Meissner and Young (1980. *J. Biol. Chem.* 255:6814–6819) and Somlyo et al. (1981. *J. Cell Biol.* 90:577–594) that a proton flux from the myoplasm into the SR supplies a portion of the electrical charge balance required as Ca^{2+} is released from the SR into the myoplasm. A comparison of the amplitude of ΔpH_{app} with that of $\Delta[Ca_T]$ indicates that, in response to a single action potential, 10–15% of the charge balance required for Ca^{2+} release may be carried by protons.

Address reprint requests to Dr. S. M. Baylor, Department of Physiology, University of Pennsylvania Medical Center, Philadelphia, PA 19104-6085.

Dr. Pape's current address is Department of Cellular and Molecular Physiology, Yale University School of Medicine, 333 Cedar Street, New Haven, CT 06510.

Dr. Hollingworth's current address is Department of Physiological Sciences, Framlington Place, The Medical School, Newcastle upon Tyne, NE2 4HH, UK.

J. GEN. PHYSIOL. © The Rockefeller University Press · 0022-1295/90/09/0493/24 $2.00 493
Volume 96 September 1990 493–516

INTRODUCTION

The preceding paper (Hollingworth and Baylor, 1990) described the dye-related absorbance changes that can be detected from frog skeletal muscle fibers microinjected with the pH indicator phenol red and stimulated to give a single action potential or brief train of action potentials. One component (denoted by ΔpH_{app}) of the absorbance change had the properties expected if a small alkalization of myoplasm occurs in conjunction with the release of Ca^{2+} from the sarcoplasmic reticulum (SR). However, another explanation for ΔpH_{app}, namely, that it reflects an event related to the rise in myoplasmic calcium concentration and not a true myoplasmic pH change, was not ruled out.

This paper describes the results of a set of experiments designed to distinguish between these two possibilities. In addition to phenol red, fibers were injected with relatively large concentrations (0.5–1.5 mM in myoplasm) of fura-2 (Grynkiewicz et al., 1985). At such buffering concentrations, fura-2 transiently binds large concentrations (0.2–0.4 mM) of the Ca^{2+} released from the SR in response to electrical stimulation; as a result, the quantity of released Ca^{2+} is increased, while the myoplasmic free $[Ca^{2+}]$ transient ($\Delta[Ca^{2+}]$) is reduced and abbreviated (Baylor and Hollingworth, 1988). Thus, in these circumstances an increase in ΔpH_{app} would be expected if ΔpH_{app} reflects a myoplasmic pH transient associated with SR Ca^{2+} release, whereas a decrease would be expected if the phenol red signal is a consequence, artifactual or otherwise, of $\Delta[Ca^{2+}]$. The increase in ΔpH_{app} that was observed supports the hypothesis that there is a myoplasmic alkalization associated with Ca^{2+} release from the SR.

A possible mechanism underlying the alkalization is that it arises as a result of a proton flux from the myoplasm into the SR in response to an SR membrane potential change created by the movement of Ca^{2+} from the SR into the myoplasm (Meissner and Young, 1980; Somlyo et al., 1981; Baylor et al., 1982*b*). If so, the measurements imply that the proton permeability averaged over the SR membrane must be extremely large, in the range 10–100 cm/s, if the hypothesized proton flux takes place at the 10^{-7} molar proton concentration of myoplasm.

A summary of some of the results has been published previously in abstract form (Pape et al., 1989).

METHODS

Intact single twitch fibers, dissected from semitendinosus or iliofibularis muscles of *Rana temporaria*, were used throughout. The phenol red absorbance signals were measured and analyzed as previously described (Baylor and Hollingworth, 1990; Hollingworth and Baylor, 1990).

Simultaneous Use of Phenol Red and Fura-2

The main goal of the present experiments was to compare the amplitude of the phenol red ΔpH_{app} signal measured in fiber regions that contained fura-2 at nonbuffering concentrations (<0.1 mM) with that measured in other regions of the same fiber that contained much larger fura-2 concentrations (as high as 1.5 mM). To this end, single fibers were injected with phenol red in two locations, usually separated by ~1 mm. For one injection, the micropipette

contained phenol red alone at the usual concentration (10–30 mM), whereas for the other injection, the pipette contained 10–30 mM phenol red plus 10–20 mM fura-2 (penta-potassium salt; Molecular Probes Inc., Eugene, OR). Myoplasmic fura-2 concentrations were quantified as previously described (Baylor and Hollingworth, 1988), from the fura-2-related resting fluorescence and from the fura-2-related absorbance and fluorescence changes recorded in response to electrical stimulation.

The analysis of the experiments was carried out under the assumption that there is no chemical interaction between phenol red and fura-2. The validity of this assumption was tested and confirmed by the following in vitro measurements:

(*a*) In a solution of (in mM) 138 KCl, 9.6 PIPES (sodium salt of piperazine-*N*,*N*-bis(2-ethane-sulfonic acid), 0.29 phenol red, and 0.30 fura-2 (pH 7.10, 22°C), in which nearly all of the fura-2 molecules were in the Ca^{2+}-free form, the dye-related absorbance spectrum of the solution was not significantly different from the sum of the two individual dye spectra measured in the identical buffer solution but containing either dye alone.

(*b*) In solutions of closely similar composition (pH 7.11, ionic strength 0.15 M, 23°C) except that they also contained 10 mM EGTA and added Ca^{2+} such that free [Ca^{2+}] was either 150 nM or saturating (~1 mM), again no significant difference was observed between the absorbance spectrum of both dyes and the sum of the absorbance spectra measured with phenol red or fura-2 alone. (For these solutions, free [Ca^{2+}] was calculated under the assumption that apparent dissociation constants (K_d) of 224 and 135 nM, respectively, apply to the Ca^{2+}-EGTA reaction (Martell and Smith, 1974) and the Ca^{2+}-fura-2 reaction (Grynkiewicz et al., 1985), at pH 7.11 and 23°C).

(*c*) The fluorescence intensity of fura-2 (excited at 420 ± 5 nm; emission collected at 510 ± 5 nm) measured in 150 nM free [Ca^{2+}] in the presence of phenol red was not significantly different from that measured in the absence of phenol red, if correction was made (cf. Eq. 5 of Baylor et al., 1981) for phenol red's absorbance of the excitation light (at 420 nm) and the emitted light (at 510 nm).

Even if phenol red and fura-2 do not interact chemically, in fibers that contain both phenol red and fura-2, the dye-related absorbance change measured at 420 nm during fiber activity may not be entirely attributable to fura-2, since phenol red's absorbance at 420 nm may also change in response to a change in myoplasmic pH. It is expected (Hollingworth and Baylor, 1990) that the amplitude of the isotropic $\Delta A(420)$ from phenol red should be about one-third that of $\Delta A(570)$. From this it was estimated that the contribution of the phenol red $\Delta A(420)$ was no more than 3% of the total dye-related $\Delta A(420)$ for the cases where the myoplasmic phenol red concentration was less than five times that of fura-2. However, in the case of one measurement from one fiber region, phenol red concentration was 22 times higher than that of fura-2 (3.07 vs. 0.14 mM). In this case, it was estimated that ~9% of the measured dye-related absorbance change at 420 nm was due to phenol red; this contamination in turn implies a 10% overestimate of Δ[Ca-fura-2], the change in concentration of the Ca^{2+}-bound form of fura-2. However, even in this worse case, the estimated change in total Ca^{2+} concentration released by the sarcoplasmic reticulum (see Methods), was likely to be overestimated by only 2%. Thus, in general, no correction was made to the $\Delta A(420)$ records before estimation of Δ[Ca-fura-2].

Proton release by fura-2. In the Discussion, a quantitative estimate is made of possible myoplasmic pH changes due to proton release from fura-2 in exchange for Ca^{2+} complexation by the dye. For this purpose, two in vitro estimates were made of the quantity of protons released by fura-2 in response to Ca^{2+} binding. For these measurements, the buffer solution contained 100 mM KCl, 1 mM PIPES (which has a pK for protons of 6.8 at 20°C) and either 0.87 or 1.89 mM fura-2 (pH 7.00, 20°C). In the first case, at 0.87 mM fura-2, solution pH measured after addition of $CaCl_2$ to a final concentration of 2.0 mM was 6.90; in the second

case, at 1.89 mM fura-2, solution pH after addition of 3.5 mM $CaCl_2$ was 6.83. After each Ca^{2+} addition, a certified stock of KOH (Aldrich Chemical Co., Milwaukee, WI) was used to titrate solution pH back to 7.00, and the total quantity of protons released from fura-2 due to Ca^{2+} binding was taken as the amount of OH^- added in the presence of fura-2 minus that added in an analogous titration carried out in the absence of fura-2. For the two cases, the calculated ratio of H^+ released to Ca^{2+} bound was 0.06 and 0.04, respectively. Thus, we have used the ratio 0.05 to estimate the quantity of protons released into the myoplasm from fura-2 in exchange for Ca^{2+} bound by the indicator (cf. Discussion).

Theoretical Calculations of Ca^{2+} Movements between SR and Myoplasm

The kinetic model (model 2) of Baylor et al. (1983), modified slightly as described in Baylor and Hollingworth (1988), was used to estimate the total concentration of Ca^{2+} (denoted by $\Delta[Ca_T]$) released from the SR into the myoplasm during activity, as well as to estimate $(d/dt)\Delta[Ca_T]$, the flux of Ca^{2+} from the SR into the myoplasm. Most of the model calculations used a calibration of the myoplasmic free $[Ca^{2+}]$ transient (denoted by $\Delta[Ca^{2+}]$) that was four times larger than that directly inferred from indicator dissociation constants measured in salt solutions that lacked myoplasmic constituents of larger molecular weight. These latter constituents appear to bind most Ca^{2+} indicator dyes and this binding probably produces an erroneously small estimate of $\Delta[Ca^{2+}]$ (Maylie et al., 1987*a*, *b*, *c*; Konishi et al., 1988). The factor of four scaling represents a somewhat arbitrary attempt to correct for this error. Model calculations were also carried out with both larger (10×) and smaller (1×) scalings of $\Delta[Ca^{2+}]$ in order to check that the principal conclusions were not strongly affected by the exact scaling chosen for $\Delta[Ca^{2+}]$.

As described in the Discussion, calculations were also carried out to simulate the SR Ca^{2+} pump reaction mechanism and associated binding of Ca^{2+} by the pump. For this purpose the reaction cycle of Fernandez-Belda et al. (1984) was used.

RESULTS

Resting pH in Fura-2-injected Muscle Fibers

The principal goal of this work was to evaluate how the presence of large concentrations of fura-2 in myoplasm might alter possible pH signals detected from phenol red in response to electrical stimulation. The first question of interest, however, was to see if the presence of fura-2 in myoplasm detectably altered the phenol red estimate of resting myoplasmic pH (denoted by pH_{app}; see Baylor and Hollingworth, 1990). In the 10 fibers of this study, which contained various concentrations of fura-2 (0–1.5 mM) at the site of pH_{app} measurement, the mean value (±SEM) of pH_{app} was 7.02 (±0.03). This value is slightly lower than the mean value of pH_{app} reported in the preceding paper, 7.17 (±0.08). The lower average value found in this study might reflect the fact that fibers were subjected to two impalements (and injections) rather than the single impalement used in the previous study. The main conclusion, however, is that the presence of fura-2 did not greatly alter the resting phenol red absorbance signal.

Signals from Phenol Red and Fura-2 during Fiber Activity

It was also found (data not shown) that in muscle fibers that contained both small and large concentrations of fura-2, changes in phenol red's isotropic absorbance

initiated by action potential stimulation had a wavelength dependence indistinguishable from that observed in the absence of fura-2 (Hollingworth and Baylor, 1990). Moreover, in fibers that contained small fura-2 concentrations (<0.1 mM), the times to half-peak and peak of the isotropic $\Delta A(570)$ signal from phenol red lagged those of the simultaneously measured intrinsic birefringence signal by 1.9 ± 0.1 ms (mean ± SEM, $n = 6$) and 7.3 ± 0.7 ms, respectively, and the peak value of $\Delta A(570)$ corresponded to a ΔpH_{app} of 0.0026 ± 0.0002 ($n = 7$). Since these values are closely similar to those observed for phenol red signals measured in the absence of fura-2 (2.4 ± 0.2 ms, 8.4 ± 0.5 ms, and 0.0025 ± 0.0002, respectively; Hollingworth and Baylor, 1990), the phenol red active signals were also not affected significantly by small myoplasmic concentrations of fura-2.

On the other hand, in fibers injected with large concentrations of fura-2 (>0.5 mM), ΔpH_{app} was 0.0038 ± 0.0002 (mean ± SEM, $n = 9$), an average value nearly 50% higher than that obtained at the low concentrations of fura-2. This increase in amplitude of ΔpH_{app}, which was observed without a significant change in the times to half-peak or to peak of the signal, was statistically significant ($P < 0.01$, two-tailed t test); its importance will be considered in detail below (Figs. 3 and 4).

Fig. 1 *A* shows examples of original optical traces recorded from a fiber region that contained phenol red (1.14 mM) and a large concentration of fura-2 (0.98 mM). The top pairs of traces, labeled 570 and 630, are the polarized transmission signals measured at 570 and 630 nm, respectively, with two forms of linearly polarized light. The phenol red isotropic $\Delta A(570)$ signal, i.e., ΔpH_{app}, obtained from these traces is shown in Fig. 1 *C* (continuous trace). The calibrated peak value of this signal was 0.0038 pH units.

The trace in Fig. 1 *A* labeled ΔB is the intrinsic birefringence signal recorded from the same fiber region. The downward component of this signal has an earlier time to peak (6.4 ms) and a smaller peak amplitude, (-0.63×10^{-3} $\Delta I/I$) than corresponding values measured in other fibers in the absence of fura-2 (time to peak, 8–10 ms; peak value, -1 to -3×10^{-3} $\Delta I/I$). Similar effects of large fura-2 concentrations on the early component of the birefringence signal were observed previously and are attributable to the Ca^{2+} buffering action of large myoplasmic concentrations of fura-2 (Baylor and Hollingworth, 1987, 1988). The lowermost trace in Fig. 1 *A* shows the change in the myoplasmic Ca^{2+}-fura-2 concentration (denoted by Δ[Ca-fura-2]). This trace has a very large peak amplitude, 0.39 mM, indicating that fura-2 in fact complexed a large concentration of myoplasmic Ca^{2+}. Moreover, the half-width of the Δ[Ca-fura-2] signal, 185 ms, is markedly prolonged in comparison with the 50–60-ms value observed in fibers that contained small fura-2 concentrations, a difference also expected from the buffering action of the dye (Baylor and Hollingworth, 1988).

Fig. 1 *B* compares the time course of the Δ[Ca-fura-2] signal (continuous trace) with that of the myoplasmic free [Ca^{2+}] transient (Δ[Ca^{2+}]; dotted trace) calculated from Δ[Ca-fura-2] by the procedure described in the legend of Fig. 1. The peak value, half width, and time to peak of Δ[Ca^{2+}] were 4.8 μM (after the fourfold scaling described in Methods), 4.3 ms, and 4.8 ms, respectively. These values are within the range observed in previous fura-2 experiments carried out in the presence of antipyrylazo III, a metallochromic Ca^{2+} indicator that appears to track Δ[Ca^{2+}] with

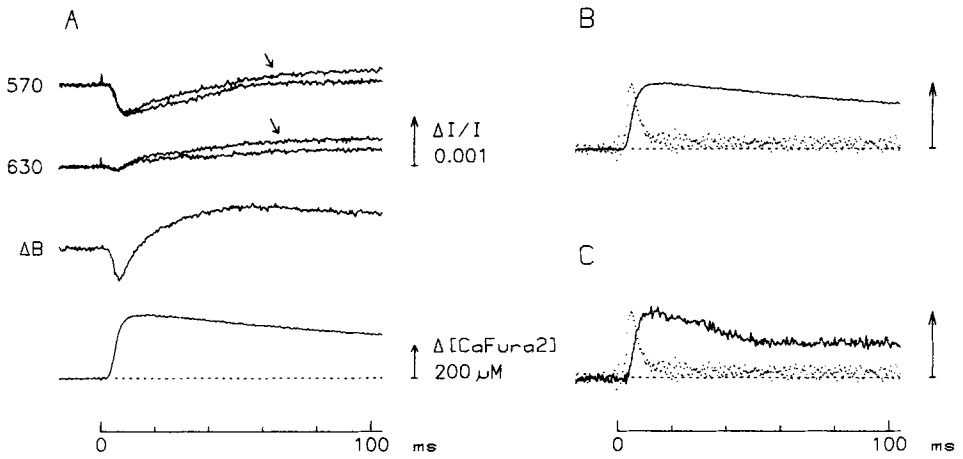

FIGURE 1. *A*, Optical signals recorded during activity from a fiber that contained 1.14 mM phenol red and a large buffering concentration of fura-2 (0.98 mM). The upper two pairs of traces, labeled 570 and 630, are transmission changes recorded with light polarized parallel (0°; arrowed traces) and perpendicular (90°) to the fiber axis at wavelengths 570 and 630 nm, respectively. The trace labeled ΔB is the intrinsic birefringence signal recorded at long wavelength (700 nm). The calibration bar (labeled $\Delta I/I$) applies to these five traces. The lowermost trace is a fura-2 fluorescence signal, calibrated in terms of Δ[Ca-fura-2] by the method described in Baylor and Hollingworth (1988). *B*, Temporal comparison of the fura-2 fluorescence signal (continuous trace) and the derived myoplasmic free $[Ca^{2+}]$ transient (dotted trace). For the calculation of $\Delta[Ca^{2+}]$, the fluorescence signal from part *A* was first calibrated in terms of Δf, the fractional change in Ca^{2+} occupancy of fura-2 (the calibration arrow in *B* corresponds to $\Delta f = 0.371$); from Δf, $\Delta[Ca^{2+}]$ was calculated (cf. Hollingworth and Baylor, 1986) under the assumption that the Ca^{2+}-fura-2 reaction in myoplasm arises as a single site response with an effective "on" rate constant of $1 \times 10^8\ M^{-1}\ s^{-1}$ and an "off" rate constant of $23\ s^{-1}$, the average values reported in Baylor and Hollingworth (1988). The fractional occupancy of the site in the resting state was assumed to be 0.06. The calibration bar corresponds to a peak change in free $[Ca^{2+}]$ of 1.2 μM before correction for, or 4.8 μM after correction for, the likely underestimate of $\Delta[Ca^{2+}]$ due to binding of the indicator to myoplasmic constituents of large molecular weight (see Methods). *C*, Temporal comparison of the phenol red–ΔpH_{app} signal (continuous trace) and the $[Ca^{2+}]$ transient from part *B* (dotted trace). The 570-nm isotropic absorbance change of phenol red (ΔpH_{app}) was obtained from the transmission records in part *A*, as described in Hollingworth and Baylor (1990); the calibration bar corresponds to +0.0038 for ΔpH_{app}. The optical measurements were made with either a 65-μm spot of light (for absorbance) or a vertical slit of 90 μm width (for birefringence and fluorescence), positioned 150 μm from the site of dye injection. Fiber 062988.1; 22–25 min after dye injection; fiber diameter, 92 μm; sarcomere length, 4.0 μm; 16.4°C.

a small (1–2 ms) kinetic delay (Baylor et al., 1985; Maylie et al., 1987*a*). The maintained elevation of $\Delta[Ca^{2+}]$ apparent at later times in Fig. 1 *B* is also similar to that observed in the previous experiments (Baylor and Hollingworth, 1988).

Fig. 1 *C* shows a temporal comparison of $\Delta[Ca^{2+}]$ (dotted trace) and ΔpH_{app} (continuous trace). The times to half-peak and peak of the ΔpH_{app} signal are delayed

by ~2.5 and 8.4 ms, respectively, compared with those of $\Delta[Ca^{2+}]$. This delay is similar to the delay between ΔpH_{app} and the intrinsic birefringence signal observed in fibers not containing fura-2 (Hollingworth and Baylor, 1990).

Fig. 2 *A* shows results from a fiber simultaneously injected with both antipyrylazo III and a large buffering concentration of fura-2 (but no phenol red). This experiment provides a methodological check that $\Delta[Ca^{2+}]$ calculated from the Δ[Ca-fura-2] signal by the procedure used in Fig. 1 agrees closely with what would be measured with antipyrylazo III after correction of the latter signal for the 1–2-ms

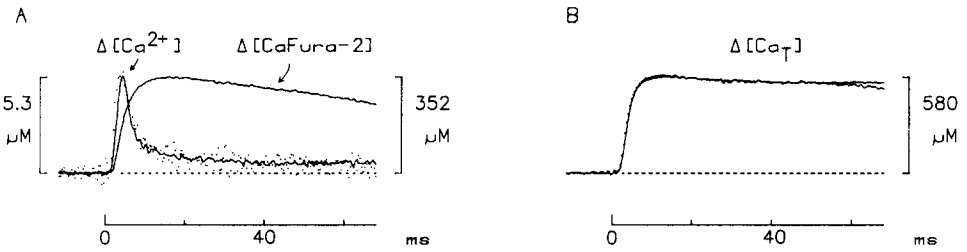

FIGURE 2. Example of the uncertainty associated with estimation of the free $[Ca^{2+}]$ transient (*A*) and total Ca^{2+} released from the SR (*B*) from measurements with fura-2 alone, as assessed from a fiber injected with both fura-2 and antipyrylazo III. *A*, The trace labeled Δ[CaFura-2] is a measured fura-2 fluorescence transient, calibrated at the right in terms of the amount of Ca^{2+}-dye complex. The dotted trace labeled $\Delta[Ca^{2+}]$ was calculated from Δ[Ca-fura-2], as described in the legend of Fig. 1, and includes the factor of 4 scaling to correct for likely errors in the calibrated value of $\Delta[Ca^{2+}]$ due to binding of fura-2 to intracellular constituents (see Methods). For the calculation of $\Delta[Ca^{2+}]$, the fractional occupancy of fura-2 by Ca^{2+} was assumed to be 0.06 in the resting state and to reach a peak value of 0.45 during activity; the latter value is set by the observed peak change in fura-2 fluorescence divided by the resting fluorescence. The use of the average rate constants given in Baylor and Hollingworth (1988) to predict $\Delta[Ca^{2+}]$ evidently worked satisfactorily, since the continuous trace labeled $\Delta[Ca^{2+}]$, which was obtained from the antipyrylazo III absorbance change measured simultaneously, and the dotted trace are very similar. The amplitude of $\Delta[Ca^{2+}]$ calculated from antipyrylazo III (cf. Baylor and Hollingworth, 1988) was also scaled fourfold. *B*, Comparison of the modeled parameter, $\Delta[Ca_T]$ (which corresponds to the total concentration of Ca^{2+} released from the SR), based on use of the two versions of the free $[Ca^{2+}]$ transient shown in part *A*; the dotted trace in *B* was obtained from the dotted trace in *A*. Fiber 090587.1; antipyrylazo III concentration, 0.63 mM; fura-2 concentration, 0.78 mM; sarcomere length, 3.8 μm; fiber diameter, 95 μm; temperature, 16°C.

delay between $\Delta[Ca^{2+}]$ and the absorbance change reported by antipyrylazo III. Both amplitude and time course of $\Delta[Ca^{2+}]$ estimated from the two dyes are very similar (superimposed dotted and continuous traces in Fig. 2 *A*, obtained from fura-2 and antipyrylazo III, respectively). Again, the brief half-width (3.9 ms) of the fast phase of the $[Ca^{2+}]$ transient, as well as the maintained phase seen at later times, are characteristic of $[Ca^{2+}]$ transients observed in the presence of large fura-2 concentrations.

It was also found in the present study that in fibers containing nonperturbing concentrations of fura-2 (<0.1 mM), $\Delta[Ca^{2+}]$, calculated as in Fig. 1 from Δ[Ca-fura-2], was essentially identical to that determined previously in fibers that contained antipyrylazo III alone (Baylor and Hollingworth, 1988). For example, the times to peak, half-widths, and peak amplitudes of $\Delta[Ca^{2+}]$ calculated from fura-2 at nonperturbing indicator concentrations were 5.5 ± 0.4 ms, 12.9 ± 1.2 ms, and 7.6 ± 0.5 μM (mean ± SEM, $n = 6$), respectively, which are not significantly different from the values 6.3 ± 0.5 ms, 14.2 ± 1.8 ms, and 7.3 ± 0.6 μM reported by Baylor and Hollingworth (1988) from antipyrylazo III measurements. These results indicate that, over a wide range of fura-2 concentrations, the procedure used in this paper for calculation of $\Delta[Ca^{2+}]$ is consistent with the previously reported experiments. Moreover, as shown in Fig. 2 *B*, any small uncertainty in the estimate of $\Delta[Ca^{2+}]$ (e.g., as in Fig. 2 *A*) resulted in a negligible difference in the estimate of the amplitude and time course of the total concentration of Ca^{2+} released from the SR into the myoplasm ($\Delta[Ca_T]$), as calculated by the computer model described in Methods.

Effects of Buffering Concentrations of Fura-2 on ΔpH_{app}, $\Delta[Ca^{2+}]$, and $\Delta[Ca_T]$

As mentioned above, the average amplitude of the phenol red ΔpH_{app} signal measured in the presence of large concentrations of fura-2 (>0.5 mM) was increased significantly in comparison with that measured at small fura-2 concentrations (<0.1 mM). Since it had been determined previously (Baylor and Hollingworth, 1988) that $\Delta[Ca_T]$ increased while peak $\Delta[Ca^{2+}]$ decreased at these large fura-2 concentrations, the tentative conclusion follows that ΔpH_{app} is not related to $\Delta[Ca^{2+}]$ itself, but is likely to be related to the amount of Ca^{2+} released from the SR. However, since the ΔpH_{app} signal shows considerable fiber-to-fiber variation (cf. Table I of Hollingworth and Baylor, 1990), measurements were carried out to estimate ΔpH_{app} at various fura-2 concentrations, and hence various values of $\Delta[Ca_T]$ within the same fiber. Such measurements were possible because of the concentration profiles established for the two indicators along the fiber axis as a result of the injection procedure (see Methods).

Fig. 3 shows examples of the relevant measurements, obtained from two fiber regions that contained quite different fura-2 concentrations (*A*, 0.09 mM; *B*, 0.80 mM). Through time to peak, the time courses of the ΔpH_{app} signals (upper traces) were very similar, but there was a clear difference in the shape of the falling phase of the signals. This latter difference is probably attributable to different contributions of movement-related components to the later time course of the absorbance transients. The ΔpH_{app} signal in *A* may have been affected less by fiber movement than that in *B*, since the fiber had been slightly stretched, from sarcomere length 3.8 to 4.0 μm, between the two measurements. This small stretch reduced the amplitude of an obvious movement artifact in the later falling phase of the birefringence signal (not shown) but did not cause any change in the rising phase of the birefringence signal; this in turn suggests that the stretch itself produced little or no change in SR Ca^{2+} release. (The continuous trace in Fig. 1 *C* provides another example of the shape observed for the falling phase of a ΔpH_{app} signal recorded at a high fura-2 concentration.) The main point to note concerning the ΔpH_{app} traces in Fig. 3 is that

the peak value in *B*, 0.0042, was nearly 60% larger than the 0.0027 value observed in *A* at the small fura-2 concentration.

Fig. 3 also shows estimates of SR Ca^{2+} movements obtained from the kinetic model (cf. Methods), which used as its input the $\Delta[Ca^{2+}]$ transients (bottom traces) calculated from the Δ[Ca-fura-2] signals (second traces from the bottom) measured from the two fiber regions. In comparison with the $\Delta[Ca^{2+}]$ trace observed in *A* in the presence of the small fura-2 concentration, $\Delta[Ca^{2+}]$ in *B* showed a clear reduction in peak height (6.0 vs. 9.2 μM) as well as a marked abbreviation in signal half width (3.7 vs. 14.8 ms). As mentioned above, this change is expected from the

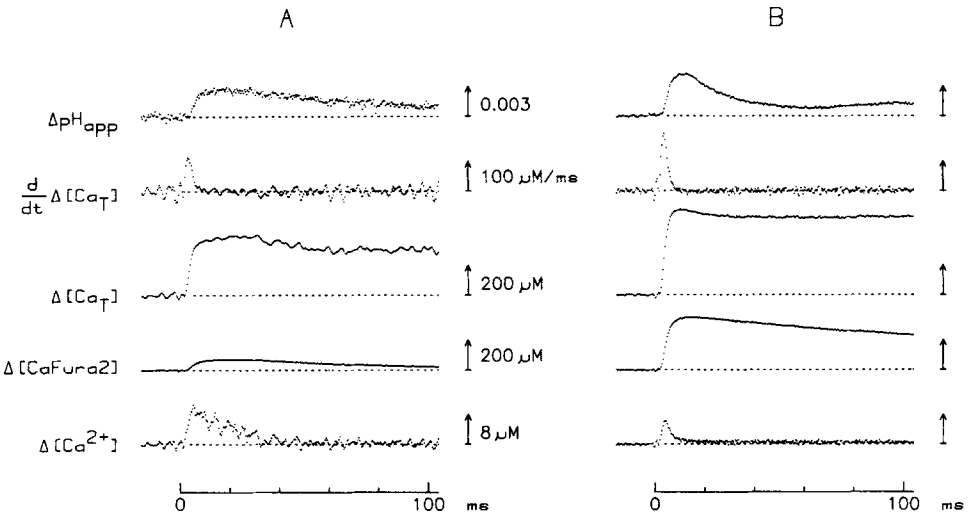

FIGURE 3. Examples of measured (ΔpH_{app} from phenol red, Δ[Ca-fura-2] from fura-2) and computed ($[d/dt]\Delta[Ca_T]$, $\Delta[Ca_T]$, and $\Delta[Ca^{2+}]$) signals obtained from two recording sites, separated by 1,000 μm, in the same fiber. $\Delta[Ca^{2+}]$ was calculated from Δ[Ca-fura-2] by the method described in the legend of Fig. 1 and includes the factor of 4 scaling. The $\Delta[Ca_T]$ and $(d/dt)\Delta[Ca_T]$ traces were then obtained from the kinetic model of SR Ca^{2+} movements, as described in Methods. Absorbance was measured with a horizontal slit of 59 μm width and 300 μm length, whereas fluorescence was collected from the full fiber width and a 300 μm length. Fiber 120886.1; fiber diameter, 83 μm; sarcomere length, 4.0 μm for part *A* and 3.8 μm for part *B;* 16.6°C. In part *A*, the phenol red and fura-2 concentrations were 0.34 and 0.09 mM, respectively; in part *B* the concentrations were 1.08 and 0.80 mM, respectively.

Ca^{2+}-buffering effects of the large myoplasmic concentration of fura-2. In contrast, SR Ca^{2+} release (traces labeled $(d/dt)\Delta[Ca_T]$ and $\Delta[Ca_T]$) was increased in the presence of the high concentration of fura-2, with peak values of 184 μM/ms vs. 117 μM/ms calculated for $(d/dt)\Delta[Ca_T]$, and 567 μM vs. 384 μM for $\Delta[Ca_T]$ (*B* and *A*, respectively). Thus, the comparison between these two fiber regions revealed a positive correlation between the amplitude of ΔpH_{app} and that of SR Ca^{2+} release, but a negative correlation between the amplitude of ΔpH_{app} and that of $\Delta[Ca^{2+}]$.

The left side of Fig. 4 (*A* and *C*) summarizes results from two fibers in which it was possible to measure ΔpH_{app} and $\Delta[Ca_T]$ from fiber regions that contained concentra-

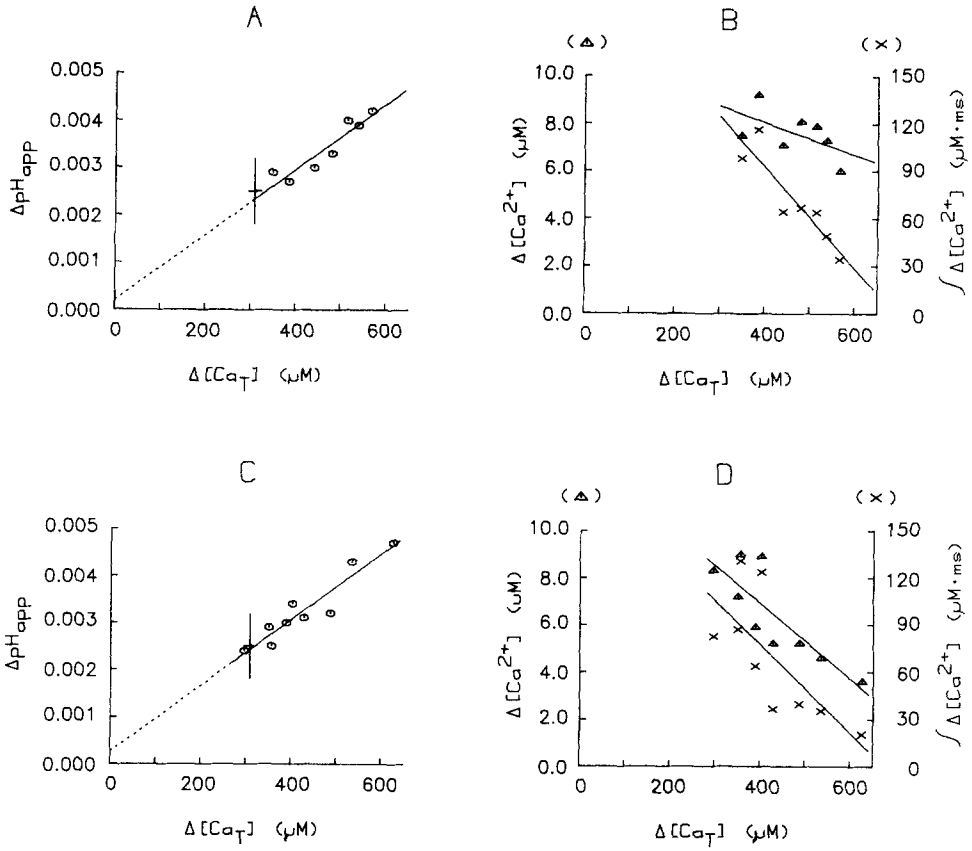

FIGURE 4. Dependence of the ΔpH_{app} signal from phenol red and the $\Delta[Ca^{2+}]$ signal from fura-2 on the modeled quantity $\Delta[Ca_T]$, which varied monotonically with the total concentration of fura-2 (not shown). For all panels the amplitudes of $\Delta[Ca^{2+}]$ were scaled by the usual factor of 4 before carrying out the model calculations. *A* and *C*, peak amplitudes of the ΔpH_{app} signals (ordinate) vs. $\Delta[Ca_T]$, as observed in two different fibers. Vertical and horizontal bars show ±1 standard deviation about the mean value of ΔpH_{app} and $\Delta[Ca_T]$, respectively, as observed in populations of fibers containing phenol red alone (Hollingworth and Baylor, 1990) or fura-2 alone (Baylor and Hollingworth, 1988). *B* and *D*, peak amplitude (triangles) and the time integral (up to 20 ms after stimulation; crosses) of $\Delta[Ca^{2+}]$ plotted vs. $\Delta[Ca_T]$, obtained from the same fibers and runs as *A* and *C*, respectively. The solid lines in *A–D* are least-squares fits to the corresponding set of data points from each fiber; in *A* and *C* the lines have been extrapolated by dashes. *A* and *B*, fiber 120886.1; fiber diameter, 81–83 μm; sarcomere length, 3.8–4.0 μm; 16.3–16.6°C; optical measurements were made between 0 and 1,000 μm from the fura-2 injection site; 16–117 min after dye injection. *C* and *D*, fiber 062988.1; fiber diameter, 87–92 μm; sarcomere length, 3.6–4.1 μm; 16.3–17.0°C; optical measurements were made between 0 and 1,250 μm from the fura-2 injection site; 10–55 min after dye injection. See Table I for slope and *y* intercept values of the fitted lines, range of dye concentrations, range of resting pH values, etc.

tions of fura-2 that varied over a wide range. In these fibers, the maximal fura-2 concentrations were sufficiently large that the observed peak values of $\Delta[Ca_T]$ were nearly twice that seen in fibers studied under the same recording conditions but in the absence of fura-2. (The average value [±SD] of $\Delta[Ca_T]$ recorded in fibers not containing fura-2 is indicated in Fig. 4, *A* and *C* by the small horizontal bar located near position 300 μM on the abscissa). ΔpH_{app} showed an approximately linear dependence on $\Delta[Ca_T]$ in these two fibers as well as in the three other fibers in which it was possible to make similar measurements over a range of fura-2 concentrations. Columns *8* and *9* of Table I summarize slope and intercept parameters for the lines that provided a best least-squares fit to the data obtained in each of the five experiments. The average values for the slopes and *y* intercepts were 6.86 (±0.08) M^{-1} and 0.0002 (±0.0001), respectively. Since the average value of the *y* intercepts is close to 0, the increment in ΔpH_{app} accompanying the increment in $\Delta[Ca_T]$ was in approximately the same proportion as the scaling constant that related these two variables at nonbuffering concentrations of fura-2.

Data from an additional five fibers also supported the existence of a clear positive correlation between ΔpH_{app} and $\Delta[Ca_T]$, although the ranges of $\Delta[Ca_T]$ in these fibers were not sufficiently wide to allow a reliable estimate of the slopes and *y* intercepts in the individual experiments. However, the best fit of a single line to the combined data from these fibers yielded slope and intercept values of 7.10 M^{-1} and 0.0002, respectively, which are closely similar to those obtained from the individual experiments given in Table I.

In Fig. 4, *B* and *D*, the symbols show the relationship between either the peak value of $\Delta[Ca^{2+}]$ (triangles, referred to the left-hand ordinate) or the integrated amplitude of $\Delta[Ca^{2+}]$ (crosses, referred to the right-hand ordinate) and the peak value of $\Delta[Ca_T]$. These data were obtained from the same runs analyzed in *A* and *C*, respectively. The best-fitted lines in *B* and *D* all show negative slopes, with a steeper slope (in a proportional sense) observed for the integral of $\Delta[Ca^{2+}]$ compared with the peak of $\Delta[Ca^{2+}]$. Quantitatively similar results were seen in the other experiments (columns *10* and *11* of Table I). Thus, $\Delta[Ca^{2+}]$ (either peak value or integrated amplitude) and ΔpH_{app} changed in opposite directions as a function of $\Delta[Ca_T]$. This finding argues against the possibility that ΔpH_{app} is primarily related to an event driven by $\Delta[Ca^{2+}]$, since a larger ΔpH_{app} was found in the presence of a smaller and briefer $\Delta[Ca^{2+}]$.

Fig. 5 compares the time courses of the ΔpH_{app} and $\Delta[Ca_T]$ signals from the same experimental runs as shown in Fig. 3. Since there is uncertainty in the absolute calibration of $\Delta[Ca^{2+}]$ (cf. Maylie et al., 1987*a, b, c*), model calculations of $\Delta[Ca_T]$ were carried out for this comparison with $\Delta[Ca^{2+}]$ scaled by three different factors: 1-, 4- and 10-fold (labeled, respectively, 1× , 4× , and 10×). In Fig. 5, the rising phase of ΔpH_{app} slightly lags that of $\Delta[Ca_T]$, for the fiber regions that contained both small (*A*) and large (*B*) concentrations of fura-2. The comparisons also show that the estimated lag becomes larger as the scaling factor for $\Delta[Ca^{2+}]$ is increased. For example, for the 1×, 4×, and 10× scalings, the time to half-peak of the ΔpH_{app} signals lagged that of $\Delta[Ca_T]$ by just under 1 ms, 1.2–1.6 ms, and 1.6–2.2 ms, respectively. The main conclusion from Fig. 5, however, is that the finding of a close

TABLE I

Dependence of ΔpH_{app} and $\Delta[Ca^{2+}]$ on $\Delta[Ca_T]$, as Estimated from Fibers Containing a Range of Fura-2 Concentrations

Fiber	[Phenol red]	pH_{app}	ΔpH_{app}	[Fura-2]	$\Delta[Ca^{2+}]$	$\Delta[Ca_T]$	ΔpH_{app}		$\Delta[Ca^{2+}]$ peak, slope	$\Delta[Ca^{2+}]$ area, slope
							Slope	Intercept		
	mM			*mM*	*μM*	*mM*	M^{-1}		*mM/μM*	*mM ms per μM*
1	2	3	4	5	6	7	8	9	10	11
120886.1	0.24–1.08	6.93–7.07	0.0027–0.0042	0.06–0.80	9.2–6.0	0.35–0.57	6.91	0.0002	−6.8	−311
120986.3	0.58–3.07	6.77–6.92	0.0025–0.0040	0.14–1.07	9.0–5.0	0.39–0.58	7.02	−0.0001	−15.7	−269
062988.1	0.15–1.64	6.84–6.96	0.0024–0.0047	0.04–1.50	9.0–3.6	0.30–0.63	7.01	0.0003	−16.1	−279
032789.1	0.47–0.64	6.95–7.05	0.0031–0.0041	0.07–0.57	8.0–5.2	0.35–0.50	6.79	0.0007	−19.5	−428
032789.2	0.33–2.54	7.01–7.06	0.0015–0.0035	0.02–0.61	8.3–5.5	0.30–0.53	6.58	−0.0001	−12.7	−190
MEAN (±SEM)							6.86 ±0.08	0.0002 ±0.0001	−14.2 ±2.1	−295 ±39

Column *1* gives the fiber reference, and columns *2–7* the range of values estimated, respectively, for the phenol red concentration in myoplasm, the resting pH_{app}, the peak change in pH_{app}, the fura-2 concentration, the peak change in free $[Ca^{2+}]$, and the peak value computed by the modeling procedure for the rise in total myoplasmic $[Ca^{2+}]$. All changes refer to the result of a single stimulated action potential. Columns *8* and *9* give the values of slope and *y* intercept for the best-fitted straight line that related the ΔpH_{app} and $\Delta[Ca_T]$ data obtained from the same fiber (cf. Fig. 4, *A* and *C*). The data selected for these fits included all runs within the same fiber for which the resting values of pH_{app} fell within a reasonably narrow range (average deviation, ±0.05 pH units). Columns *10* and *11* give the slope of the best-fitted straight line that related, respectively, the peak value of $\Delta[Ca^{2+}]$ and $\Delta[Ca_T]$ (cf. Fig. 4, *B* and *D*, triangles) and the integrated amplitude of $\Delta[Ca^{2+}]$ (up to 20 ms after stimulation) and $\Delta[Ca_T]$ (cf. Fig. 4, *B* and *D*, crosses).

coincidence between the rising phases of ΔpH_{app} and $\Delta[Ca_T]$ also supports the conclusion that ΔpH_{app} is related to $\Delta[Ca_T]$.

Effects of Fura-2 on the Phenol Red Active Dichroic Signal

The phenol red active dichroic signal (Hollingworth and Baylor, 1990) was also examined to see if signal amplitude changed in the presence of the larger concentrations of fura-2. If the dichroic signal is driven by $\Delta[Ca^{2+}]$ (cf. Baylor et al., 1982*a*; Hollingworth and Baylor, 1990), its amplitude should decrease with increasing fura-2 concentrations, i.e., vary inversely with $\Delta[Ca_T]$ (cf. Fig. 4, *B* and *D*). Because of

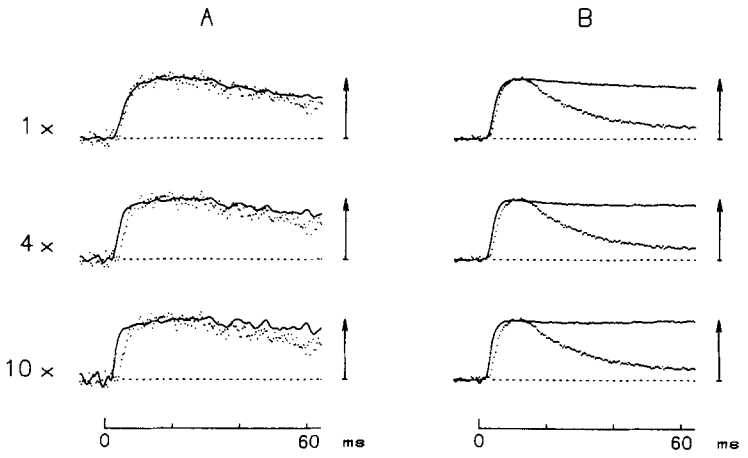

FIGURE 5. Temporal comparison between ΔpH_{app} signals (dotted traces, from phenol red) and $\Delta[Ca_T]$ signals (continuous traces, from fura-2) measured in the presence of a small (0.09 mM, part *A*) or large (0.80 mM, part *B*) concentration of fura-2. The records were obtained from the same runs as in Fig. 3, *A* and *B*. Peak ΔpH_{app} was 0.0027 in *A* and 0.0042 in *B*. In both parts, $\Delta[Ca_T]$ signals were calculated from the model, but with $\Delta[Ca^{2+}]$ left unscaled (top traces, labeled 1×), scaled 4-fold (middle traces, labeled 4×) or scaled 10-fold (bottom traces, labeled 10×). For the comparison of time courses, the ΔpH_{app} and $\Delta[Ca_T]$ signals have been displayed with the same vertical amplitudes. In *A* and *B*, respectively, peak $\Delta[Ca_T]$ was 290 and 449 μM for the 1× scaling, 384 and 567 μM for the 4× scaling, and 433 and 619 μM for the 10× scaling. In *B*, a movement artifact probably contributes to the relatively rapid falling phase of ΔpH_{app} (see text).

the small size of the dichroic signal and the necessity to measure this signal at the shorter wavelengths (e.g., 480 or 450 nm), only 4 of the 10 fibers in this study contained reliable information on this point. The most information, as well as the clearest result, was obtained in one fiber, for which the fura-2 concentration varied between 0.14 and 1.07 mM and the phenol red concentration between 0.58 and 3.07 mM. As the estimates of $\Delta[Ca_T]$ for the various fiber regions increased, from 0.39 to 0.58 mM, the normalized amplitude of the dichroic signal ($[\Delta A_0 - \Delta A_{90}]/[(A_0 + 2A_{90})/3]$, measured at 480 nm) decreased approximately linearly, from 1.38×10^{-3} to 0.73×10^{-3}. Moreover, in the three other fibers, the normalized

amplitude of the 480-nm dichroic signal was 0.70 (±0.02) × 10^{-3} at times when the average value (±SEM) of $\Delta[Ca_T]$ was 0.49 (±0.04) mM. The value 0.70 × 10^{-3} is approximately one-third that observed in fibers not containing fura-2 (Hollingworth and Baylor, 1990). Thus, the combined results support the hypothesis that the phenol red dichroic signal, in contrast to the phenol red isotropic signal, is due to a change in a dye binding reaction that is sensitive to myoplasmic free $[Ca^{2+}]$, since the dichroic amplitude and $\Delta[Ca^{2+}]$ both appear to be reduced by large concentrations of fura-2.

DISCUSSION

The principal experimental findings of this paper are: (*a*) large myoplasmic concentrations of fura-2 increase the amplitude of the ΔpH_{app} signal detected with phenol red, and (*b*) the increase in amplitude of ΔpH_{app} appears to be proportional to the extra sarcoplasmic reticulum Ca^{2+} release that arises because of the presence of fura-2 (Table I and Fig. 4, *A* and *C*). Moreover, since the increase in ΔpH_{app} occurred in the presence of a smaller and briefer free $[Ca^{2+}]$ transient (Table I and Fig. 4, *B* and *D*), the results strongly argue that ΔpH_{app} is not a consequence of the rise in myoplasmic $[Ca^{2+}]$ itself. These findings support the interpretation that the apparent alkalization reported by phenol red reflects a real change in myoplasmic pH and that this change is closely related to the amount of Ca^{2+} released from the SR. A tentative explanation is that ΔpH_{app} reflects the movement of protons from the myoplasm into the SR in electrical exchange for Ca^{2+} released into the myoplasm (cf. Meissner and Young, 1980; Somlyo et al., 1981; Baylor et al., 1982*b*).

Possible Contributions to ΔpH from Myoplasmic Binding Events

This section considers how myoplasmic changes unrelated to a proton movement into the SR might contribute to the measured ΔpH_{app}.

H^+ release by fura-2. As described in Methods, when fura-2 complexes Ca^{2+} at pH = 7.00, the ratio of protons released to Ca^{2+} ions bound is ~0.05. Thus, during a muscle Ca^{2+} transient, protons released from fura-2 probably make some contribution to ΔpH_{app}, a contribution that is expected to vary according to the amplitude and time course of Δ[Ca-fura-2]. Since Δ[Ca-fura-2] was measured in the experiments, the total concentration of protons released to the myoplasmic pool from fura-2 can be estimated as 0.05 × Δ[Ca-fura-2]. This quantity, in turn, can be converted to ΔpH units (referred to as ΔpH_{fura}) by division by the myoplasmic buffering power (assumed to be 33 meq of protons per liter of myoplasm per pH unit, the average of the values reported by Bolton and Vaughan-Jones, 1977; Abercrombie et al., 1983; and Curtin, 1986). Finally, ΔpH_{fura} may be subtracted from the phenol red ΔpH_{app} signal to obtain an estimate of the myoplasmic pH change not associated with protons contributed by fura-2.

Fig. 6 *A* shows a reanalysis of the data in Fig. 4 *A* after calculation and subtraction of ΔpH_{fura} from ΔpH_{app}. The data points have a greater vertical displacement at the higher values of $\Delta[Ca_T]$, which in turn correspond to larger values of Δ[Ca-fura-2] and therefore more proton release from fura-2. Consequently, the least-squares line fitted to the data in Fig. 6 *A* has a steeper slope as well as a more negative intercept

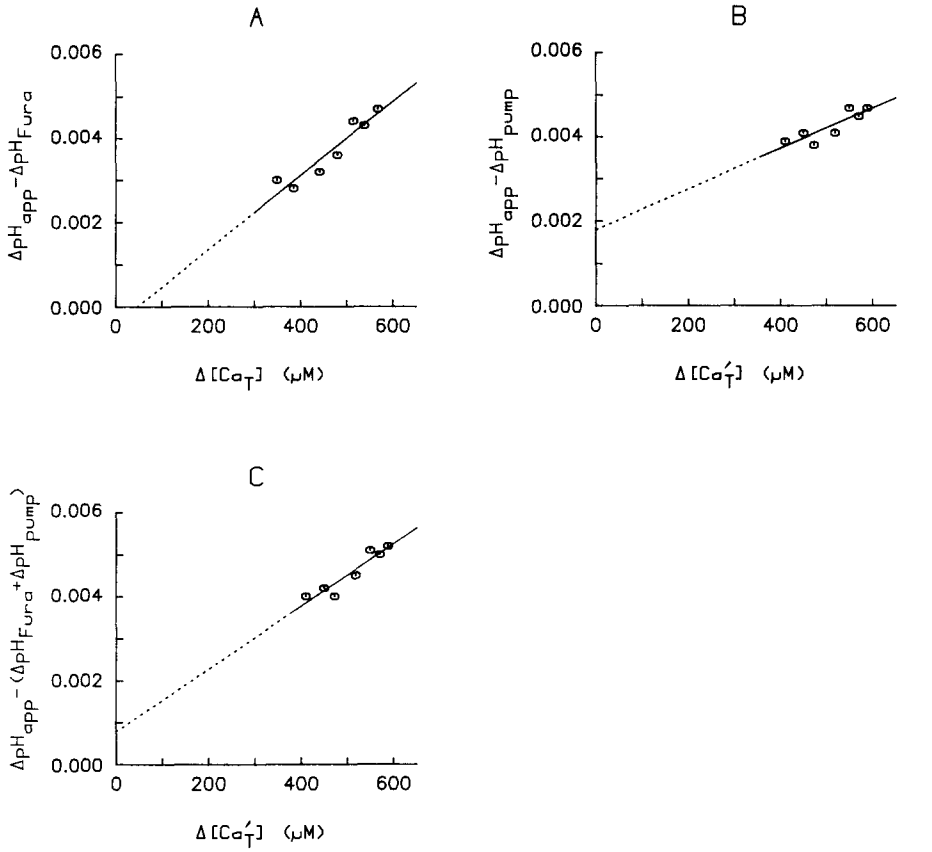

FIGURE 6. Relationship between the total concentration of Ca^{2+} released into the myoplasm (abscissa) and the myoplasmic pH change estimated from the phenol red ΔpH_{app} signal (ordinate) after correction for the effect of protons released from myoplasmic Ca^{2+} binding sites. Data in Fig. 4 *A* were replotted after correction for the pH change expected due to the release of protons from: (*A*) fura-2 itself (ΔpH_{fura}); (*B*) SR Ca^{2+} pump sites (ΔpH_{pump}); and (*C*) both fura-2 and the Ca^{2+} pump. For the modeling, $\Delta[Ca^{2+}]$ was scaled by the factor of 4 for all panels, and, additionally, Ca^{2+} bound to Ca^{2+} pump sites of the SR was taken into account in calculating $\Delta[Ca'_T]$ in *B* and *C* (see text). In each part, the indicated line is the least-squares fit to the data points. Slope and intercept values were 8.8 M^{-1} and −0.0004, 4.9 M^{-1} and 0.0018, and 7.5 M^{-1} and 0.0008, respectively, for *A*, *B*, and *C*. Fiber 120886.1. For additional details, see text and the legend of Fig. 4.

on the ordinate. The main point to note is that a clear positive correlation is still observed between the two variables. Thus, inclusion of proton release by fura-2 in the analysis does not change the qualitative conclusion given in the first paragraph of the Discussion.

H^+ Release from Intrinsic Ca^{2+} Binding Sites. When Ca^{2+} binds to receptor sites normally present in myoplasm, such as on parvalbumin, troponin C, and the SR Ca^{2+} pump, protons might also be released into the myoplasm and thus contribute to the measured ΔpH_{app}. The contribution to ΔpH_{app} from parvalbumin is probably

negligible, since the concentration of metal-free parvalbumin sites is probably no more than 50–100 μM and there appears to be a minimal release of protons associated with Ca^{2+} binding to these sites (maximum of 0.02–0.06 mol H^+ released per mol Ca^{2+} bound at pH 7.0 [Tanokura and Yamada, 1985; see also Ogawa and Tanokura, 1986]). Similarly, the contribution from the troponin regulatory sites is probably also quite small, since, in the case of troponin C, the ratio of protons released to Ca^{2+} ions bound is reported to be 0.01–0.06 mol per mol (Potter et al., 1977; Yamada and Kometani, 1982; Imaizumi et al., 1987) and, in the case of whole troponin, the ratio also appears to be very close to zero and possibly negative (Yamada et al., 1976; see also Ogawa, 1985). Chiesi and Inesi (1980), however, report that the binding of Ca^{2+} to the transport sites of the SR Ca^{2+} pump does release protons, with one proton released per Ca^{2+} bound at pH 6.0. Watanabe et al. (1981) suggest a value of 7.3 for the apparent pK of the ionizable group at the metal binding site and we have chosen this pK, in combination with a myoplasmic pH of 7.0, for the analysis that follows. With these assumptions, the ratio of protons released to Ca^{2+} ions bound by the transport sites is 0.67.

To make a quantitative estimate of the amplitude and time course of the concentration of protons released by the pump, we have used the 11-step Ca^{2+} transport reaction cycle proposed by Fernandez-Belda et al. (1984). The total concentration of pump molecules, referred to the myoplasmic water volume, was taken as 120 μmol/liter (=240 μM Ca^{2+} transport sites; Baylor et al., 1983). The rate constants for the individual reaction steps were adjusted from 25 to 16.5°C under the assumption of a Q_{10} of 3.0, which is the value reported for the Q_{10} of the initial (Ogawa et al., 1981) and maximal (Weber et al., 1966) uptake rates of the pump. For the calculations, we have assumed the following values for reactant concentrations: adenosine triphosphate (ATP), 5 mM; adenosine diphosphate, 0.01 mM; inorganic phosphate, 1 mM; myoplasmic resting [Ca^{2+}], 0.02 μM; SR luminal [Ca^{2+}], 1 mM. Under these conditions, which are appropriate for a fiber at rest, the steady-state distribution of the enzyme (E) is nearly all (98.8%) in the E·ATP state (cf. Fernandez-Belda et al., 1984). In response to a sudden increase in myoplasmic [Ca^{2+}], the enzyme distributes to the initial Ca^{2+}-bound states and then moves sequentially through the remaining reaction steps.

Trace *b* of Fig. 7 *A* shows a sample calculation of the concentration of Ca^{2+} removed as a function of time from the myoplasmic pool by the Ca^{2+} pump if the kinetic reaction is driven by the increase in myoplasmic free [Ca^{2+}] shown in trace *d*. This latter trace was obtained from a Δ[Ca-fura-2] measurement by means of the procedure described in Results (cf. Fig. 1). On the time scale shown, nearly all of the Ca^{2+} captured by the pump is the result of the early binding steps in the reaction cycle, with <1% of the Ca^{2+} having been translocated to the luminal side (reaction step 6) by 40 ms after stimulation. As discussed above, the quantity and time course of protons released into the myoplasmic pool from the Ca^{2+} pump may be approximated as 0.67 times trace *b*. Trace *c* in Fig. 7 *A* is the $\Delta[Ca_T]$ waveform calculated by the usual modeling procedure (as in Figs. 2–5 and 6 *A*) and represents the net increase in myoplasmic Ca^{2+} concentration, i.e., Ca^{2+} not associated with the SR. Trace *a*, on the other hand, which is the sum of traces *b* and *c*, represents the

concentration of Ca^{2+} released from the SR into the myoplasm including that recaptured by the pump. This quantity is denoted below as $\Delta[Ca'_T]$. In principle, this trace should reach a peak value and thereafter remain constant. Since the trace actually decays slightly at later times, there must be some inaccuracy in one or more aspects of the modeling procedures. On the time scale of interest, however, this inaccuracy is not large.

Fig. 7 *B* shows several estimates of the change in myoplasmic pH associated with the release of Ca^{2+} from the SR, from the same experimental run as considered in

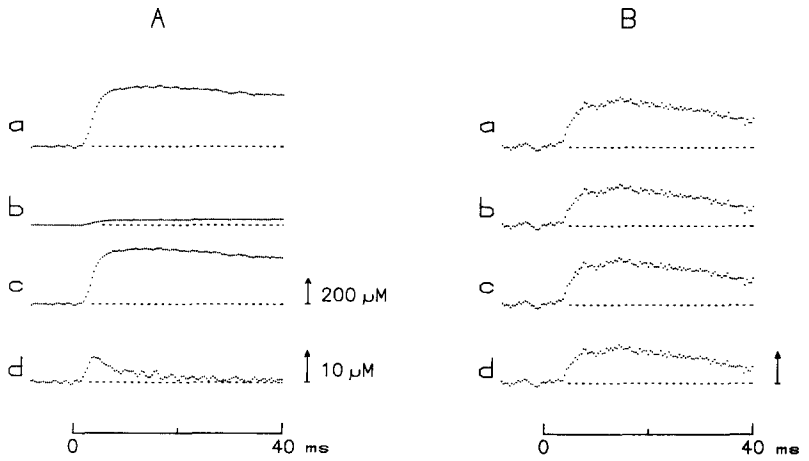

FIGURE 7. *A*, Kinetic modeling of Ca^{2+} movements, including Ca^{2+} binding to the sarcoplasmic reticulum Ca^{2+} pump. Trace *d*, $\Delta[Ca^{2+}]$ obtained from a Δ[Ca-fura-2] signal (not shown) and scaled by a factor of 4. Trace *c*, $\Delta[Ca_T]$, excluding Ca^{2+} bound to the SR Ca^{2+} pump, i.e., as calculated in Results (cf. Fig. 3). Trace *b*, Ca^{2+} removed from the myoplasm by the SR Ca^{2+} pump, as estimated from the model of Fernandez-Belda et al. (1984), integrated by a fourth-order Runge-Kutta routine. Trace *a*, $\Delta[Ca_T]$ after correction for the Ca^{2+} removed by the SR Ca^{2+} pump, i.e., the sum of traces *b* and *c*. The 200-μM calibration arrow applies to traces *a–c*. *B*, Different estimates of the myoplasmic ΔpH signal associated with SR Ca^{2+} release. The calibration bar represents a ΔpH of 0.003. Trace *d*, the ΔpH_{app} signal directly measured by phenol red. Traces *a–c*, the ΔpH_{app} signal corrected for the protons released from the SR Ca pump (*c*), from fura-2 (*b*), and from both the Ca^{2+} pump and fura-2 (*a*). *A* and *B* were obtained from the same experimental run. Fiber 120886.1; sarcomere length, 3.8 μm. The concentrations of phenol red and fura-2 were 0.61 mM and 0.32 mM, respectively.

Fig. 7 *A*. Trace *d*, with peak value of 0.0033, is simply ΔpH_{app}, i.e., the phenol red $\Delta A(570)$ calibrated by means of Fig. 1. Trace *c*, peak values 0.0041, is ΔpH_{app} minus the pH change associated with proton release from the SR Ca^{2+} pump (i.e., plus trace *b* in Fig. 7 *A* after multiplication by 0.67 and division by the myoplasmic buffering power). The late phase of trace *c* shows proportionally less recovery than that of trace *d*, suggesting that some of the rapid recovery observed in the uncorrected ΔpH_{app} signal may be due to release of protons from the SR Ca^{2+} pump. Trace *b*, peak value 0.0036, is ΔpH_{app} minus the pH change associated with the estimated proton release from fura-2 (Δ[Ca-fura-2] trace not shown in Fig. 7 *A*).

Trace *a*, peak value 0.0045, is ΔpH_{app} corrected for the protons released both from the pump and from fura-2; thus, this trace represents the myoplasmic pH change that may directly reflect the net movement of protons from the myoplasm into the SR in exchange for the release of Ca^{2+} from the SR into the myoplasm. Through time to peak, this trace has a time course closely similar to either $\Delta[Ca_T]$ or $\Delta[Ca'_T]$ (traces *c* and *a*, respectively, in Fig. 7 *A*; cf. Fig. 5).

Fig. 6, *B* and *C* summarize the results of this analysis applied to all the runs shown in the experiment of Fig. 4 *A*. In Fig. 6 *B*, the ordinate shows ΔpH_{app} corrected for pump protons alone (correction denoted by ΔpH_{pump}), and the abscissa is expressed in terms of $\Delta[Ca'_T]$ ($\Delta[Ca_T]$ plus $[Ca^{2+}]$ recaptured by the pump). The least-squares fitted line has a reduced, but still positive, slope in comparison with that in Figs. 4 *A* and 6 *A*. In Fig. 6 *C*, the ordinate reflects the correction for both ΔpH_{pump} and ΔpH_{fura} (and the abscissa is again expressed in terms of $\Delta[Ca'_T]$). The best-fitted line to this data set also shows a clear positive correlation between ΔpH and $\Delta[Ca'_T]$. This relationship should probably be considered the one most directly relevant to the hypothesis that protons carry a portion of the charge balance associated with SR Ca^{2+} release. Independent of the exact method of analysis, however, the qualitative conclusions are that: (*a*) the amplitude of the proton movement appears to be positively correlated with the amount of Ca^{2+} released from the SR, and (*b*) the time course of the proton movement is similar to that of the increase in total calcium concentration.

Other possible contributions to ΔpH. Chemical reactions in myoplasm are also a potential source or sink for protons. ATP hydrolysis and the accompanying liberation of phosphate as $H_2PO_4^-$ should release protons, whereas rephosphorylation of ADP coupled to the hydrolysis of phosphocreatine should generate $HPO_4^{=}$ and therefore remove protons from myoplasm. The quantitative effects of these phosphate reactions, however, are probably not significant in the experiments on the rapid time scale of Fig. 7. For example, phosphate release due to cross-bridge attachment should be negligible at the site of optical recording, where the sarcomere length was 3.6–4.1 μm. (The small twitch tension observed in the experiments (cf. Fig. 3 of Hollingworth and Baylor, 1990), which was typically no more than a few percent of the twitch tension recorded at normal sarcomere length, presumably arises from force generation in a few sarcomeres located near the tendon attachments, where overlap of thick and thin filaments is still significant in the highly stretched fiber; Huxley and Peachey, 1961). Moreover, as mentioned above, the concentration of Ca^{2+} transported to the luminal side of the SR by the Ca^{2+} pump reaction was computed to be negligible on the time scale of Fig. 7; therefore phosphate liberation and its associated pH change, due to energy consumption by the pump, is probably also negligible. Although the possibility cannot be excluded that other chemical reactions may generate or absorb significant quantities of protons, most metabolic events subsequent to Ca^{2+} release probably take place on a slower time scale than shown in Fig. 7 and therefore can probably be ignored.

Influence of Other Model Parameter Selections on the Estimation of ΔpH. Also considered was how the relationship shown in Fig. 6 *C* might vary with alternative parameter selections used in the model. A number of such calculations were carried out (data not shown) and, over a reasonable range of parameter choices, a clear

positive correlation between $\Delta pH_{app} - (\Delta pH_{fura} + \Delta pH_{pump})$ and $\Delta[Ca'_T]$ remained. Parameter selections for these calculations included: (*a*) a change in the scaling of $\Delta[Ca^{2+}]$, including 1× and 10× ; (*b*) an increase in the pK of the ionizable site on the pump from 7.3 to 9.0; and (*c*) a 10-fold increase in all the rate constants for the Ca^{2+} pump reaction. Thus, the conclusion that an increased myoplasmic proton loss (exclusive of fura-2 and the SR Ca^{2+} pump) is associated with an increased release of Ca^{2+} from the SR is not strongly model dependent in these calculations. However, not all possible combinations of parameter selections gave a clear positive correlation, as in Fig. 6. For example, if the extreme assumptions were made that proton release by fura-2 is negligible, that the Ca^{2+} pump sites release one proton per Ca^{2+} bound, and that a 10× scaling of $\Delta[Ca^{2+}]$ applies, the correlation between the corrected ΔpH_{app} and $\Delta[Ca'_T]$ was only barely positive. Moreover, if it was also assumed that, with activation, sites on the thin filament release a significant quantity of protons in exchange for bound Ca^{2+}, a significant negative correlation was observed between the two variables. Release of protons with thin filament activation might be considered a possibility, since the binding of Ca^{2+} to myofibrils from skinned skeletal muscle fibers is reported to be pH sensitive in the range 6.2–7.0 (Blanchard et al., 1984). However, as pointed out by these authors, their finding could reflect pH effects on several processes, including an interaction between actin and myosin. Metzger and Moss (1988), for example, have suggested that the reduced sensitivity of the myofilaments to Ca^{2+} at low pH reflects an inhibitory effect of protons on cross-bridge attachment, with resultant changes in the affinity of the thin filament for Ca^{2+} (cf. Bremel and Weber, 1972; Gordon and Ridgway, 1987; Guth et al., 1987). Thus, there is no strong evidence to favor the interpretation that, at the long sarcomere lengths used in our experiments, binding of Ca^{2+} to the myofilaments is associated with the release of protons to the myoplasmic pool.

Proton Movement as a Fraction of the Ca^{2+} Movement

A linear correlation, similar to that in Fig. 6 *C*, was also found to describe the results of the other experiments after analogous corrections were made to the data. The average values (±SEM) of the slopes and *y* intercepts for the least-squares fitted lines to the five individual experiments analyzed by the method of Fig. 6 *C* were 7.5 (±0.3) M^{-1} and +0.0006 (±0.0001), respectively. This average slope, when multiplied by the myoplasmic buffering power (33 meq of protons per liter per pH unit) and the ratio of charges on the two ions (0.5), indicates that the early myoplasmic alkalization would be explained if ~12% of the Ca^{2+} released from the SR is electrically counter-balanced by the movement of protons from myoplasm to SR. This percentage may be compared with the 30–45% "charge deficit" reported by Somlyo et al. (1981) and Kitazawa et al. (1984), who made measurements, by means of the electron probe technique, of the ionic content of the terminal cisternae of the SR at the end of a 1.2-s tetanus. Given the very different experimental techniques as well as types of stimulation used, our conclusions and those of Somlyo et al. (1981), implicating proton movements between myoplasm and SR, appear to be in reasonable agreement.

Deductions Concerning the Proton Permeability of the SR Membrane

The hypothesized flux of protons from myoplasm to SR can be used to calculate an apparent proton permeability (denoted by P_{H+}) averaged over the SR membrane. For this calculation we have assumed that: (*a*) the proton concentration is the same (10^{-7} M) on both luminal and myoplasmic sides of the membrane, as would be expected if H^+ distribution is in electro-chemical equilibrium with an SR resting membrane potential close to 0 mV (cf. Somlyo et al., 1977, 1981); (*b*) the proton movement during activity is driven by a transient change in SR membrane potential, denoted by ΔV (myoplasm relative to lumen), created by the movement of Ca^{2+} down its electro-chemical gradient into the myoplasm; and (*c*) the proton flux across the SR membrane obeys the constant-field current equation (Goldman, 1943). Then:

$$P_{H^+} = \frac{RT}{F \cdot \Delta V} \frac{M_{H^+}}{[H^+]}, \tag{1}$$

where R, T, and F have their usual meaning and M_{H^+} denotes the flux of protons (in moles per second per square centimeter of SR membrane) from the myoplasm into the SR (cf. Eq. 3 of Baylor et al., 1984). From the average peak value of $(d/dt)\Delta pH_{app}$, 0.61×10^{-3} ms^{-1}, calculated from 11 fibers that contained either no Ca^{2+} indicator or a nonperturbing concentration of Ca^{2+} indicator, the peak rate of decrease of the total myoplasmic proton concentration was 20 μM ms^{-1} (0.61×10^{-3} ms^{-1} times myoplasmic buffering power). Hence, according to Eq. 1, P_{H^+} is 10–100 cm/s, if ΔV is assumed to be 10 to 1 mV, respectively (cf. Oetliker, 1982; Baylor et al., 1984; Garcia and Miller, 1984) and if the density of SR membranes is taken as 5×10^4 cm^2 of membrane per cm^3 of myoplasmic H_2O (the average of the values 7.6×10^4/cm and 2.8×10^4/cm reported by Peachey [1965] and Mobley and Eisenberg [1975]; see Baylor et al. [1983] for referral of units to myoplasmic H_2O volume). Even given the order of magnitude uncertainty for the value assumed for ΔV, the values calculated for P_{H^+} are extremely large. For example, even 10 cm/s is only about an order of magnitude smaller than the proton permeability of a 50-Å water layer (the approximate thickness of a membrane). This follows since D_{H^+}, the diffusion coefficient of protons in water, is $\sim 8 \times 10^{-5}$ cm^2/s at 20°C (see, for example, Hille, 1984), so that $D_{H^+}/50$ Å = 160 cm/s.

Several values are given in the literature for the proton permeability of the SR membrane, based on fluorescence measurements from isolated SR vesicles. Meissner and Young (1980), who used a membrane-potential sensitive dye and exposed vesicles to variable inside and outside concentrations of H^+ and K^+, report a lower limit of 10^{-3} cm/s for P_{H^+}. Although this limit is some four to five orders of magnitude below the values calculated above, resolution of a larger permeability value was not possible given the kinetic limitations of the technique. In contrast, Nunogaki and Kasai (1986), who used a fluorescent pH indicator and a stopped-flow apparatus with millisecond time resolution, report that P_{H^+} is 11 cm/s, a value within the range calculated above.

If the apparent P_{H^+} for the SR membrane is on the order of one-tenth that expected for a 50-Å water layer, one wonders how such a large effective permeability could come about. One possibility might be that 10% of the area of the SR

membrane is made up of water-filled pathways that provide the diffusional area for the large P_{H^+}. It seems highly unlikely that the usual sort of ion channel could be the source of such a large diffusional area, since >90% of the protein integral to the SR membrane is reported to be Ca^{2+} pump protein (Meissner, 1975; Fleischer, 1985), which exists at a density of $\sim 2 \times 10^4$ molecules per μm^2 (Scales and Inesi, 1976). Moreover, even if each pump molecule contained a water-filled pore that permitted diffusion of protons (but not Ca^{2+} and probably not other ions), it seems likely that the total area of such water-filled pores within all the pump molecules would comprise less than 1% of the SR membrane area. However, it is possible that the movement of protons across the membrane, in either channels or pumps, might proceed by a "hydrogen-bonded chain" mechanism (Nagle and Tristram-Nagle, 1983; cf. Eisenberg and Kauzmann, 1969; Onsager, 1969). According to this idea, propagated changes in hydrogen bonding in an ordered chain of H_2O molecules permits rapid H^+ (or OH^-) transfers. For example, such a mechanism may explain (cf. Deamer, 1987) the anomalously high proton permeability observed in the gramicidin A channel, where the ratio of proton permeability to sodium permeability (Myers and Haydon, 1972) or to potassium permeability (Deamer, 1987) has been reported to be 132 and 5×10^4, respectively, i.e., between 20 and 10^4 times higher than that expected from the relative ion mobilities in solution. Thus, with the increased proton permeability expected from such a mechanism, the requisite fraction of SR membrane area given over to water-filled pathways in either channels or pumps might be much less than 1%.

Another consideration relevant to the calculation of P_{H^+} from Eq. 1 is that the supply of protons to the proton-permeable pathways might not depend simply on the free $[H^+]$ concentration (assumed to be 10^{-7} M), but might involve protons donated directly from mobile buffers (cf. "general" acid catalysis, as described, for example, in Jencks, 1969). Since millimolar concentrations of mobile buffer are normally present in myoplasm (Godt and Maughan, 1988), and were also present in the vesicle experiments of Nunogaki and Kasai (1986), the value of P_{H^+} calculated above from the free H^+ concentration might be artifactually high by several orders of magnitude.

In conclusion, physico-chemical considerations do not appear to rule out the possibility that a peak proton flux across the SR membrane of 4×10^{-10} mol s^{-1} cm^{-2}, as inferred from the phenol red isotropic signal, might occur during normal muscle activity.

We thank Dr. W. K. Chandler for a gift of a sample of phenol red and for comments on the manuscript, and Dr. J. H. Kaplan and Dr. C. Miller for discussions.

Financial support was provided by the U.S. National Institutes of Health (grant NS-17620 to S.M.B.)

Original version received 6 June 1989 and accepted version received 9 February 1990.

REFERENCES

Abercrombie, R. I., R. W. Putnam, and A. Roos. 1983. The intracellular pH of frog skeletal muscle: its regulation in isotonic solution. *Journal of Physiology.* 345:175–187.

Baylor, S. M., W. K. Chandler, and M. W. Marshall. 1981. Studies in skeletal muscle using optical probes of membrane potential. *In* Regulation of Muscle Contraction: Excitation-Contraction Coupling. A. D. Grinnell and Mary A. B. Brazier, editors. Academic Press, New York. 97–130.

Baylor, S. M., W. K. Chandler, and M. W. Marshall. 1982*a*. Dichroic components of Arsenazo III and Dichlorophosphonazo III signals in skeletal muscle fibres. *Journal of Physiology*. 331:179–210.

Baylor, S. M., W. K. Chandler, and M. W. Marshall. 1982*b*. Optical measurements of intracellular pH and magnesium in frog skeletal muscle fibres. *Journal of Physiology*. 331:105–137.

Baylor, S. M., W. K. Chandler, and M. W. Marshall. 1983. Sarcoplasmic reticulum calcium release in frog skeletal muscle fibres estimated from Arsenazo III calcium transients. *Journal of Physiology*. 344:625–666.

Baylor, S. M., W. K. Chandler, and M. W. Marshall. 1984. Calcium release and sarcoplasmic reticulum membrane potential in frog skeletal muscle fibres. *Journal of Physiology*. 348:209–238.

Baylor, S. M., and S. Hollingworth. 1987. Effect of calcium (Ca) buffering by Fura2 on the second component of the intrinsic birefringence signal in frog isolated twitch muscle fibres. *Journal of Physiology*. 391:90*P*. (Abstr.)

Baylor, S. M., and S. Hollingworth. 1988. Fura-2 calcium transients in frog skeletal muscle fibers. *Journal of Physiology*. 403:151–192.

Baylor, S. M., and S. Hollingworth. 1990. Absorbance signals from resting frog skeletal muscle fibers injected with the pH indicator dye phenol red. *Journal of General Physiology*. 96:449–471.

Baylor, S. M., S. Hollingworth, C. S. Hui, and M. E. Quinta-Ferreira. 1985. Calcium transients from intact frog skeletal muscle fibers simultaneously injected with Antipyrylazo III and Azol. *Journal of Physiology*. 365:70*P*. (Abstr.)

Blanchard, E. M., B.-S. Pan, and R. J. Solaro. 1984. The effect of acidic pH on the ATPase activity and troponin Ca^{2+} binding of rabbit skeletal myofilaments. *Journal of Biological Chemistry*. 259:3181–3186.

Bolton, T. B., and R. D. Vaughan-Jones. 1977. Continuous direct measurement of intracellular chloride and pH in frog skeletal muscle. *Journal of Physiology*. 270:801–833.

Bremel, R. D., and A. Weber. 1972. Cooperation within actin filament in vertebrate skeletal muscle. *Nature New Biology*. 238:97–101.

Chiesi, M., and G. Inesi. 1980. Adenosine 5′-triphosphate dependent fluxes of manganese and hydrogen ions in sarcoplasmic reticulum vesicles. *Biochemistry*. 19:2912–2918.

Curtin, N. A. 1986. Buffer power and intracellular pH of frog sartorius muscle. *Biophysical Journal*. 50:837–841.

Deamer, D. W. 1987. Proton permeation of lipid bilayers. *Journal of Bioenergetics and Biomembranes*. 19:458–479.

Eisenberg, D., and W. Kauzmann. 1969. Structure and Properties of Water. Oxford University Press, New York. 296 pp.

Fernandez-Belda, F., M. Kurzmack, and G. Inesi. 1984. A comparative study of calcium transients by isotropic tracer, metallochromic indicator and intrinsic fluorescence in sarcoplasmic reticulum ATPase. *Journal of Biological Chemistry*. 259:9687–9698.

Fleischer, S. 1985. Sarcoplasmic reticulum and other membranes in the regulation of skeletal muscle contraction and relaxation. *In* Structure and Function of Sarcoplasmic Reticulum. S. Fleischer and Y. Tonomura, editors. Academic Press, New York. 119–145.

Garcia, A. M., and C. Miller. 1984. Channel-mediated monovalent cation fluxes in isolated sarcoplasmic reticulum vesicles. *Journal of General Physiology*. 83:819–839.

Godt, R. E., and D. W. Maughan. 1988. On the composition of the cytosol of relaxed skeletal muscle of the frog. *American Journal of Physiology*. 254:C591–C604.

Goldman, D. E. 1943. Potential, impedance, and rectification in membranes. *Journal of General Physiology.* 27:37–60.

Gordon, A. M., and E. B. Ridgway. 1987. Extra calcium on shortening in barnacle muscle. Is the decrease in calcium binding related to decreased cross-bridge attachment, froce, or length? *Journal of General Physiology.* 90:321–340.

Grynkiewicz, G., M. Poenie, and R. Y. Tsien. 1985. A new generation of Ca^{2+} indicators with greatly improved fluorescence properties. *Journal of Biological Chemistry.* 260:3440–3450.

Guth, K., K. Winnekes, and J. D. Potter. 1987. Further evidence that cycling crossbridges increase the Ca^{2+} affinity of TnC. *Biophysical Journal.* 51:327*a.* (Abstr.)

Hille, B. 1984. Ionic Channels of Excitable Membranes. Sinauer Associates, Inc., Sunderland, MA. 426 pp.

Hollingworth, S., and S. M. Baylor. 1986. Calcium transients in frog skeletal muscle fibers injected with Azo-1. *In* Optical Methods in Cell Physiology. P. DeWeer and B. M. Salzberg, editors. John Wiley & Sons, Inc., New York. 261–263.

Hollingworth, S., and S. M. Baylor. 1990. Changes in phenol red absorbance in response to electrical stimulation of frog skeletal muscle fibers. *Journal of General Physiology.* 96:473–491.

Huxley, A. F., and L. D. Peachey. 1961. The maximum length for contraction in vertebrate striated muscle. *Journal of Physiology.* 156:150–165.

Imaizumi, M., M. Tanokura, and K. Yamada. 1987. A calorimetric study on calcium binding by troponin C from bull frog skeletal muscle. *Journal of Biological Chemistry.* 262:7963–7966.

Jencks, W. P. 1969. Catalysis in Chemistry and Enzymology. McGraw-Hill Inc., New York. 163–170.

Kitazawa, T., A. P. Somlyo, and A. V. Somlyo. 1984. The effects of valinomycin on ion movements across the sarcoplasmic reticulum in frog muscle. *Journal of Physiology.* 350:253–268.

Konishi, M., A. Olson, S. Hollingworth, and S. M. Baylor. 1988. Myoplasmic binding of Fura-2 investigated by steady-state fluorescence and absorbance measurements. *Biophysical Journal.* 54:1089–1104.

Martell, A. E., and R. M. Smith. 1974. Critical Stability Constants. Vol. 1. Amino Acids. Plenum Publishing Corp., New York. 139–271.

Maylie, J., M. Irving, N. L. Sizto, G. Boyarsky, and W. K. Chandler. 1987*a.* Optical signals obtained with tetramethylmurexide in cut frog twitch fibers. *Journal of General Physiology.* 89:145–176.

Maylie, J., M. Irving, N. L. Sizto, and W. K. Chandler. 1987*b.* Comparison of Arsenazo III optical signals in intact and cut frog twitch fibers. *Journal of General Physiology.* 89:41–81.

Maylie, J., M. Irving, N. L. Sizto, and W. K. Chandler. 1987*c.* Optical signals obtained with Antipyrylazo III in cut frog twitch fibers. *Journal of General Physiology.* 89:83–143.

Meissner, G. 1975. Isolation and characterization of two types of sarcoplasmic reticulum vesicles. *Biochemica et Biophysica Acta.* 389:51–68.

Meissner, G., and R. C. Young. 1980. Proton permeability of sarcoplasmic reticulum vesicles. *Journal of Biological Chemistry.* 255:6814–6819.

Metzger, J. M., and R. L. Moss. 1988. Depression of Ca^{2+} insensitive tension due to reduced pH in partially troponin-extracted skinned skeletal muscle fibers. *Biophysical Journal.* 54:1169–1173.

Mobley, B. A., and B. R. Eisenberg. 1975. Sizes of components in frog skeletal muscle measured by methods of stereology. *Journal of General Physiology.* 66:31–45.

Myers, V. B., and D. A. Haydon. 1972. Ion transfer across lipid membranes in the presence of gramicidin A. *Biochemica et Biophysica Acta.* 274:313–322.

Nagle, J. F., and S. Tristram-Nagle. 1983. Hydrogen bonded chain mechanisms for proton conduction and proton pumping. *Journal of Membrane Biology.* 74:1–14.

Nunogaki, K., and M. Kasai. 1986. Determination of the rate of rapid pH equilibration across isolated sarcoplasmic reticulum membranes. *Biochemical and Biophysical Research Communications.* 140:934–940.

Oetliker, H. 1982. An appraisal of the evidence for a sarcoplasmic reticulum membrane potential and its relation to calcium release in skeletal muscle. *Journal of Muscle Research and Cell Motility.* 3:247–272.

Ogawa, Y. 1985. Calcium binding to troponin C and troponin: effects of Mg^{2+}, ionic strength and pH. *Journal of Biochemistry.* 97:1011–1023.

Ogawa, Y., N. Kurebayashi, A. Irimajiri, and T. Hanai. 1981. Transient kinetics for Ca uptake by fragmented sarcoplasmic reticulum from bullfrog skeletal muscle with reference to the rate of relaxation of living muscle. *In* Advances in Physiological Sciences. vol. 5. Molecular and Cellular Aspects of Muscle Function. E. Varga, A. Kover, T. Kovacs, and L. Kovacs, editors. Akademiai Kiado, Budapest. 416–435.

Ogawa, Y., and M. Tanokura. 1986. Steady-state properties of calcium binding to parvalbumins from bullfrog skeletal muscle: effects of Mg^{2+}, pH, ionic strength and temperature. *Journal of Biochemistry.* 99:73–80.

Onsager, L. 1969. The motion of ions: principles and concepts. *Science.* 166:1359–1364.

Pape, P. C., M. Konishi, S. Hollingworth, and S. M. Baylor. 1989. Myoplasmic pH and calcium transients from intact frog skeletal muscle fibers simultaneously injected with Phenol Red and Fura-2. *Biophysical Journal.* 55:412*a*. (Abstr.)

Peachey, L. D. 1965. The sarcoplasmic reticulum and transverse tubules of frog's sartorius. *Journal of Cell Biology.* 25:209–231.

Potter, J. D., F.-J. Hsu, and H. J. Pownall. 1977. Thermodynamics of Ca^{2+} binding to troponin C. *Journal of Biological Chemistry.* 252:2452–2454.

Scales, D., and G. Inesi. 1976. Assembly of ATPase protein in sarcoplasmic reticulum membranes. *Biophysical Journal.* 16:735–751.

Somlyo, A. V., H. Gonzales-Serratos, H. Shuman, G. McClellan, and A. P. Somlyo. 1981. Calcium release and ionic changes in the sarcoplasmic reticulum of tetanized muscle. An electron-probe study. *Journal of Cell Biology.* 90:577–594.

Somlyo, A. V., H. Shuman, and A. P. Somlyo. 1977. Elemental distribution in striated muscle and effects of hypertonicity. Electron probe analysis of cryo-sections. *Journal of Cell Biology.* 74:828–857.

Tanokura, M., and K. Yamada. 1985. A calorimetric study of Ca^{2+} binding to two major isotypes of bullfrog parvalbumin. *FEBS Letters.* 185:165–169.

Watanabe, T., D. Lewis, R. Nakamoto, M. Kurzmack, C. Fronticelli, and G. Inesi. 1981. Modulation of calcium binding in sarcoplasmic reticulum adenosinetriphosphatase. *Biochemistry.* 20:6617–6625.

Weber, A., R. Herz, and I. Reiss. 1966. Studies of the kinetics of calcium transport by isolated fragmented sarcoplasmic reticulum. *Biochemica Zeitschrift.* 345:329–369.

Yamada, K., and K. Kometani. 1982. The changes in heat capacity and entropy of troponin C induced by calcium binding. *Journal of Biochemistry.* 92:1505–1517.

Yamada, K., H. Mashima, and S. Ebashi. 1976. The enthalpy change accompanying the binding of calcium to troponin relating to the activation heat production of muscle. *Proceedings of the Japan Academy.* 52:252–255.